

KINETIC ANALYSIS OF AROMATIZATION OF N-HEXANE ON PLATINUM/ALUMINA CATALYST USING THE TIKHONOV REGULARIZATION TECHNIQUE

Oyinlola Rukayat Oresgun¹, Aramide Adenike Adesina¹ & Alfred Akpoveta Susu²

¹Department of Chemical & Polymer Engineering, Lagos State University, Epe, Lagos, Nigeria

²Department of Chemical Engineering, University of Lagos, Lagos, Nigeria

E-mail: lollykee@yahoo.com; ajeigbearamide@yahoo.com; poveta_susu@yahoo.com

ABSTRACT

Tikhonov regularization, which is a new technique for converting time-concentration data into concentration-reaction rate data, was applied to the kinetic analysis of n-hexane aromatization on Platinum/Alumina Catalyst. The technique was used for the conversion of the experimental concentration-time data to rate-concentration data. Due to the ill-posed nature of the problem of obtaining of reaction rates from experimental data, conventional methods will lead to noise amplification of the experimental data. Hence, Tikhonov regularization technique is preferably employed because it is entirely independent of reaction rate models and it also manages to minimize noise amplification, thus, leading to more reliable results. The kinetic parameters obtained by the application of the Nelder-Mead simplex optimization technique to formulated mechanistic models was used to discriminate among rival kinetic models based upon physicochemical criteria and thermodynamic tests to give the rate of conversion of adsorbed hexene-1 to adsorbed methylcyclopentane when hydrogen is adsorbed as a bi-molecular specie as the rate determining step.

Keywords: *Tikhonov regularization technique; Nelder-Mead simplex method; Hexane reforming; Mechanistic kinetic models; Kinetic and equilibrium parameters.*

1. INTRODUCTION

In the investigation of the kinetics of chemically reacting systems, it is often necessary to convert experimental time-concentration data into concentration-reaction rate data in order to determine the kinetic parameters of postulated reaction rate models. A variety of procedures has been developed to perform this task. For other reactions it may be possible to deduce the rate constants by examining the initial slope of the time-concentration data. Another approach is to modify or simplify the kinetic model if this can be physically justified. A more general technique is to treat the rate equations as ordinary differential equations. These equations are integrated to give the concentration of the reactants and products as a function of time with the rate constants appearing as unknown parameters. These parameters are then adjusted to minimize the deviation of the computed time-concentration profile from its experimentally observed counterpart.

Integration of simple rate equations can be performed analytically leading to simple expressions for the time-concentration profiles. However, for many rate equations analytical solution cannot be found and they have to be integrated numerically. Determination of the rate constants to minimize the deviation from experimental data becomes correspondingly more complicated to the extent that they cannot be determined to a reasonable degree of accuracy. Therefore, if inappropriate methods are used, the conversion procedure becomes an ill-posed problem in the sense that the noise in the original data will be amplified leading to unreliable results.

Hadamard [9] defined a linear problem to be *well posed* if it satisfies the following three requirements: (a) existence, (b) uniqueness, and (c) stability. A problem is said to be *ill-posed* if one or more of these requirements are not satisfied. Yeow et al. [3] showed that Tikhonov regularization is a reliable procedure for processing the time-concentration data of reaction kinetics. This procedure has been successful in keeping noise amplification under control and meets the important requirement that it does not require the assumption of a model to describe the original experimental data. This procedure was first used by Yeow and Taylor [4] for obtaining velocity profiles from various experimentally measured velocity data. Yeow et al. [3] carried out further application of the procedure to reactions ranging from first order reactions to chain reactions involving a number of intermediate steps with rate equation of the rate determining process. Omowunmi and Susu [5] used the Tikhonov regularization technique in converting the concentration-time data for n-eicosane pyrolysis data procured by Susu and Kunugi [6] to generate the kinetic parameters for this homogeneous autocatalytic chain reaction. In addition, Omowunmi and Susu [7] also used the same technique in determining the kinetic parameters for the reforming of n-heptane, n-heptene and 3-methylhexane on Pt/Alumina catalyst.

The aim of this paper is to more exhaustively apply Tikhonov regularization to the conversion of the concentration-time data of the complex reaction of the aromatization of n-hexane on Platinum/Alumina catalyst to concentration-rate data at temperatures 440°C, 460°C, 480°C, 500°C using the well documented experimental data from the work of Agbajelola and Aberugba [8]. Rate equations of the Langmuir-Hinselwood type will be generated and the values for the respective kinetic parameters would be generated by fitting the rate equations into the resulting concentration-reaction rate profile. Thus, the performance of this new procedure can be demonstrated by showing that these parameters conform to the expected trend in the kinetic investigation under study.

2. THE GOVERNING EQUATION

The relationship between the reaction rate $r(t)$ and the time-concentration profile $C(t)$ can be written as:

$$r(t) = \frac{dC(t)}{dt} \quad (1)$$

This can be rewritten as:

$$C(t) = \int_{t'}^t r(t') dt' + C_0 \quad (2)$$

where C_0 is the initial concentration. This equation can be regarded as a Volterra integral equation for the unknown reaction rate $r(t)$ and initial concentration C_0 if this quantity is not measured directly or if the experimental measurement is considered to be unreliable. This is an integral equation of the first kind. The mathematical nature of this equation shows that the problem of obtaining $r(t)$ is an ill-posed problem in the sense that if inappropriate methods are to inaccurate results [2].

Instead of solving Equation (2) directly for $r(t)$, this equation, through integration by parts, can be transformed into:

$$C^c(t) = \int_{t'=0}^t \left[\frac{d[t' r(t')]}{dt'} - t' f(t') \right] dt' + C_0 \quad (3)$$

$$= tr(t) - \int_{t'=0}^t t' f(t') dt' + C_0 \quad (4) \quad = t \left(\int_{t'=0}^t f(t') dt' + r_0 \right) - \int_{t'=0}^t t' f(t') dt' + C_0 \quad (5)$$

$$= \int_{t'=0}^t (t - t') f(t') dt' + C_0 + tr_0 \quad (6)$$

where $f(t) = \frac{dr(t)}{dt}$ and $r_0 = r(0)$ is the initial rate.

Equation (6) can be regarded as a Volterra integral equation of the first kind to be solved for the unknown function $f(t)$ and the constants C_0 and r_0 . Superscript C is used to distinguish the computed concentration given by this equation from its experimentally measured counterpart which will be denoted by superscript M . The computational procedure developed here will obtain C_0 and r_0 as part of the solution to the integral equation. However, if the initial concentration is exactly known, e.g. when the initial mole fraction is zero or unity, then C_0 takes on this exact value and is not treated as an unknown. Similarly if there are physical reasons to suggest that the initial reaction rate is identically zero then r_0 is assigned this value and not treated as an unknown.

Once $f(t)$, C_0 and r_0 are known, $r(t)$ and $C(t)$ can be obtained by direct numerical integration. Since numerical integration does not suffer from noise amplification, the $r(t)$ thus obtained can be expected to be relatively free from the influence of experimental noise.

Equation (6) is the starting point of the present investigation. Inputs to this equation are the experimentally measured time-concentration data points: $(t_1, C_1^M), (t_2, C_2^M), (t_3, C_3^M), \dots, (t_{N_D}, C_{N_D}^M)$. N_D is the number of points in the set and is usually a relatively small number, typically around 10 – 50. The data points may or may not be regularly spaced out in time. From the way Equation (6) was obtained it is clear that this equation is independent of the order of the reaction and its nature.

3. DISCRETIZING THE VOLTERRA INTEGRAL EQUATION

In discretized form Equation (2) becomes:

$$C_i^c = C_0 + t_i r_0 + \sum_{t_j}^{t_j'=t_i} \alpha_{ij} (t_i - t_j) f_j \Delta t'$$

$i = 1, 2, \dots, N_D, \quad j = 1, 2, \dots, N_K$ (7) where $f_1, f_2, f_3, \dots, f_{N_K}$ are the discretized $f(t)$. The independent variable $0 \leq t' \leq t_{max}$ is divided into N_K uniformly spaced discretization points with step size $\Delta t' = t_{max} / (N_K - 1)$. t_{max} is the largest t_i in the data set. α_{ij} is the coefficient arising from the numerical scheme used to approximate the integral in Eq. 2. For Simpson's $1/3$ rule, used throughout the present investigation, $\alpha_{ij} = 2/3$ for odd j (except $\alpha_{ij} = 1/3$) and $4/3$ for even j . Depending on whether the t_i of the i th experimental data point

coincides with a discretization point, the last α_{ij} associated with this point may have to be adjusted, by interpolation, to allow for fractional step size.

The deviation of C^C from C^M is given by

$$\delta_i = C_i^M - \left(C_0 + t_i r_0 + \sum_{t'_j=0}^{t'_j=t_i} \alpha_{ij} (t_i - t'_j) f_j \Delta t' \right) \quad (8)$$

$$\delta_i = C_i^M - C_i c_0 - B_i r_0 + \left(\sum_{t'_j=0}^{t'_j=t_i} \alpha_{ij} (t_i - t'_j) f_j \Delta t' \right) \quad (9)$$

or, in matrix notation, $\delta = C^M - C C_0 - B r_0 - A f$. (10)

C and B are $N_D \times 1$ column vectors and A is a $N_D \times N_K$ matrix of coefficients of the unknown column vector.

$$f = [f_1, f_2, f_3, \dots, f_{N_K}]^T. \quad (11)$$

while C, B and A are given by

$$C_i = 1 \quad (12)$$

$$B_i = t_i \quad (13)$$

$$A_{ij} = \alpha_{ij} (t_i - t'_j) \Delta t' \text{ for } t_i \geq t'_j = 0 \text{ for } t_i \leq t'_j \quad (14)$$

In Equation (14) $t_i, i = 1, 2, 3, \dots, N_D$ are the times at which the concentration is measured and $t'_j, j = 1, 2, 3, \dots, N_K$ are then uniformly discretized time $0 \leq t \leq t_{max}$. N_K generally exceeds the number of data points N_D , thus A is not a square matrix and Equation (9) cannot be inverted to give a unique $f(t), C_0$ and r_0 . Instead, these unknowns are selected to minimize the sum of squares of δ_i , i.e. to minimize

$$\sum \delta_i^2 = \delta^T \delta = (C^M - C C_0 - B r_0 - A f)^T \times (C^M - C C_0 - B r_0 - A f) \quad (15)$$

4. TIKHONOV REGULARIZATION

To obtain smooth solutions to ill-posed problems, the standard Tikhonov regularization method is most often used. Ill-posed problems are frequently encountered in science and engineering. The term itself has its origins in the early 20th century. It was introduced by Hadamard [9] who investigated problems in mathematical physics. According to his beliefs, ill-posed problems did not model real world problems, but later it appeared how wrong he was. Hadamard [9] defined a linear problem to be well posed if it satisfies the following three requirements: (a) existence, (b) uniqueness, and (c) stability. A problem is said to be ill-posed if one or more of these requirements are not satisfied. A classical example of an ill-posed problem is a linear integral equation of the first kind in $L^2(I)$ with a smooth kernel. A solution to this equation, if it exists, does not continuously depend on the right-hand side and may not be unique. When a discretization of the problem is performed, we obtain a matrix equation in C^m ,

$$k u = f \quad (16)$$

where k is an $m \times n$ matrix with a large condition number, $m \geq n$. A linear least squares solution of the system (17) is a solution to the problem

$$\min_{u \in C^n} \{ \|k u - f\|^2 + \alpha^2 \|u\|^2 \} \quad (17)$$

where the Euclidean vector norm in C^m is used. We say that the algebraic problems (16) and (17) are discrete ill-posed problems.

The numerical methods for solving discrete ill-posed problems in function spaces and for solving discrete ill-posed problems have been presented in many papers. These methods are based on the so-called regularization methods. The main objective of regularization is to incorporate more information about the desired solution in order to stabilize the problem and find a useful and stable solution. The most common and well-known form of regularization is that of Tikhonov [16]. It consists in replacing least-squares problem (17) by that with a suitably chosen Tikhonov functional. The most basic version of this method can be presented as

$$\min_{u \in C^n} \{ \|k u - f\|^2 + \alpha^2 \|u\|^2 \} \quad (18)$$

where $\alpha \in \mathbb{R}$ is called the regularization parameter. The Tikhonov regularization is a method in which the regularized solution is sought as a minimizer of a weighted combination of the residual norm and a side constraint. The regularization parameter controls the weight given to the minimization of the side constraint.

Minimizing $\delta^T \delta$ in Equation (15) will not in general result in a smooth $f(t)$ because of the noise in the experimental data. To ensure smoothness, additional conditions have to be imposed. In the present investigation, the additional condition is the minimization of the sum of squares of the second derivative $d^2 f / dt^2$ at the internal discretization points. In terms of the column vector f , this condition takes on the form of minimizing

$$\sum_{j=2}^{N_K-1} (d^2f/dt'^2)_j^2 = (\beta f)^T (\beta f) = f^T \beta^T \beta f \quad (19)$$

where β is the tri-diagonal matrix of coefficients arising from the finite difference approximation of d^2f/dt'^2

$$\beta = \begin{bmatrix} 1 & -2 & 1 & & & & & \\ & 1 & -2 & 1 & & & & \\ & & 1 & -2 & 1 & & & \\ \cdot & \cdot & \cdot & \cdot & \cdot & \cdot & \cdot & \\ \cdot & \cdot & \cdot & \cdot & \cdot & \cdot & \cdot & \\ & & & 1 & -2 & 1 & & \\ & & & & 1 & -2 & 1 & \end{bmatrix} \frac{1}{(\Delta t'^2)} \quad (20)$$

In Tikhonov regularization [2] instead of minimizing $\delta^T \delta$ and $f^T \beta^T \beta f$ separately, a linear combination of these two quantities $R = \delta^T \delta + \lambda f^T \beta^T \beta f$ is minimized. λ is an adjustable weighting/regularization factor that controls the extent to which the noise in the kinetic data is being filtered out. It balances the two requirements on $f(t)$:

- fitting the experimental data
- remaining as smooth as possible.

A large λ will give a smooth $f(t)$ but at the expense of the goodness of fit of the kinetic data and vice versa.

Minimizing R becomes:

$$\frac{\partial R}{\partial f_j} = 0 \quad j = 1, 2, \dots, N_K \quad (21)$$

$$\frac{\partial R}{\partial C_0} = 0 \quad (22)$$

$$\frac{\partial R}{\partial r_0} = 0 \quad (23)$$

These give rise to a set of linear algebraic equations for f , C_0 and r_0 (assuming that both initial conditions are unknown). It can be shown [10] that the f , C_0 and r_0 that satisfy Equations (21) to (23) are given by

$$f' = (A'^T A' + \lambda \beta'^T \beta')^{-1} A'^T C^M \quad (24)$$

For convenience f' is used to denote the column vector $[f_1, f_2, f_3, \dots, f_{N_K}, C_0, r_0]^T$ incorporating C_0 and r_0 into f . A' is the composite matrix (A, C, B) derived from Equations (21) to (23) to reflect the inclusion of C_0 and r_0 in f . Similarly β' is the composite matrix $(\beta, \mathbf{0}, \mathbf{0})$ where $\mathbf{0}$ is a $(N_K - 2) \times 1$ column vector of 0 to allow for the fact that C_0 and r_0 play no part in the smoothness condition in Equation (19). The f' given by Equation (24) can now be substituted into Equation (6) to give $C(t)$. It can also be substituted in the defining equation $dr(t)/dt = f(t)$ and integrated to give the reaction rate $r(t)$.

As $f(t)$ is known at a large number of closely spaced discretization points the integration for $r(t)$ and $c(t)$ can be carried out using any of the standard numerical integration procedures. Since integration is a smoothing process, the resulting $r(t)$ and $c(t)$ can be expected to be well-behaved smooth functions. This has been observed in all the examples investigated.

5. REGULARIZATION PARAMETER IDENTIFICATION

A suitable choice of the regularization parameter λ has to be provided by the user in order to apply Tikhonov regularization [2]. The regularization parameter controls the weight given to the minimization of the side constraint. Thus, the quality of the regularized solution is controlled by the regularization parameter. An optimal regularization parameter should fairly balance the perturbation error and the regularization error in the regularized solution.

There are several possible strategies that depend on additional information referring to the analysed problem and its solution, e.g., the discrepancy principle and the generalized cross-validation method. The discrepancy principle is an a-posteriori strategy for choosing α as a function of an error level (the input error level must be known). The generalized cross validation method is based on a-priori knowledge of a structure of the input error, which means that the errors in f can be considered to be uncorrelated zero-mean random variables with a common variance, i.e., white noise.

Another practical method for choosing α when data are noisy is the L-curve criterion [11,12]. The method is based on the plot of the norm of the regularized solution versus the norm of the corresponding residual. The practical use of such a plot was first introduced by Lawson and Hanson [13]. The idea of the L-curve criterion is to choose a regularization related to the characteristic L-shaped "corner" of the graph.

The most appropriate value of λ depends on factors such as the noise level in the experimental data, the number of data points N_D , and discretization points N_K , and the numerical schemes used to approximate the integral in Equation (6) and the second derivative in Equation (19). It is neither a property of the reaction under investigation nor a

constant determined by the concentration measurement technique or instrument employed [2]. If λ is set too small the determinant of the matrix $A^T A' + \lambda \beta^T \beta'$ in Equation (24) may become close to zero and the inverse of the matrix becomes ill conditioned. This is a manifestation of the ill-posed nature of the problem of obtaining reaction rates from time-concentration data.

6. APPLICATION TO N-HEXANE AROMATIZATION ON PLATINUM/ALUMINA CATALYST AT DIFFERENT TEMPERATURES

Agbajelola and Aberuagba [8] investigated the kinetics of hydrogen influence on n-hexane aromatization over platinum/alumina catalyst. Applying quasi-steady state approximation for the adsorbed species since conditions on the catalyst surface are stationary, the mechanistic rate equations will be obtained for the reaction, assuming eight possible rate controlling steps. The experimental data (Appendix A) to be used for discrimination among rival kinetics models for n-hexane aromatization were gathered in a pulsed microcatalytic tubular reactor with plug flow total pressure of 391.8 kPa and a temperature range of 420–500°C.

Based on the behavior of these parameters over the temperature range, the models will be discriminated to determine the model that best fits the data. The kinetic rate and equilibrium constants for all the eight kinetic models will be obtained using the optimization routine of Nelder-Mead modified simplex algorithm by minimizing the sum of squares of all errors between experimental and predicted rates. The selection criteria used were: (1) the increase and decrease with temperature of the kinetic rate and equilibrium constants, respectively, (2) statistical and thermodynamic scrutiny.

From the experimental data from this work, concentrations and reaction rates will be computed independent of the rate model by applying equations (6), (24) as described in Section 3

6.1 The step wise analysis of the conversion of concentration-time data to reaction rate-concentration data

The experimental data from the work of Agbajelola and Aberuagba [8] was presented in the form of x , the mole fraction of exit products, (n-hexane, cracked fraction, methylcyclopentane, benzene) and their concentration against the residence time (Appendix A). The data was for the reaction occurring at temperatures: $T_1 = 440^\circ\text{C}$, $T_2 = 460^\circ\text{C}$, $T_3 = 480^\circ\text{C}$, $T_4 = 500^\circ\text{C}$

The step wise analysis of the conversion of the data from concentration-time data to reaction rate-concentration data, is as follows:

$t_{\max} = 3.75$, $N_D = 5$, take $N_k = 20$

Step one: Divide the independent variable, time (t), where $0 \leq t' \leq t_{\max}$ is divided uniformly spaced discretization points N_k with step size $\Delta t' = t_{\max} / (N_k - 1)$.

Step two: Generate α_{ij} from Simpson's 1/3 rule, where $\alpha_{ij} = 2/3$ for odd j (except $\alpha_{i1} = 1/3$) and $4/3$ for every even j

Step three: Compute $(t_i - t_j')$ in Equation (14)

Step four: Compute $\Delta t'$ in Equation (14)

Step five: Compute A_{ij} using Equation (14)

Step six: Compute matrix \mathbf{A} , where \mathbf{A} is a 5×20 matrix of coefficients of unknown column vector

Step seven: Compute matrix \mathbf{C} , where \mathbf{C} is a 5×1 matrix of ones

$$\mathbf{C} = \begin{bmatrix} 1 \\ 1 \\ 1 \\ 1 \\ 1 \end{bmatrix}$$

Step eight: Compute matrix \mathbf{B} using Equation (13), where \mathbf{B} is a 5×1 matrix of t_i 's.

$$\mathbf{B} = \begin{bmatrix} t1 \\ t2 \\ t3 \\ t4 \\ t5 \end{bmatrix}$$

Step nine: Compute **A** using Equation (14)

$$A = \begin{matrix} A_{ij} \text{ Where } i=1, j=1 & \cdot & \cdot & \cdot & A_{ij} \text{ Where } i=1, j=20 \\ \cdot & \cdot & \cdot & \cdot & \cdot \\ \cdot & \cdot & \cdot & \cdot & \cdot \\ \cdot & \cdot & \cdot & \cdot & \cdot \\ A_{ij} \text{ where } i=5, j=1 & \cdot & \cdot & \cdot & A_{ij} \text{ where } i=5, j=20 \end{matrix}$$

Step ten: Compute composite matrix **A'** where

A' = **A**, **C**, **B** which is a 5 x 22 matrix

Step eleven: Compute the transpose of **A'**.

Compute **β** using Equation (20), where **β** is a tri-diagonal matrix of 20 x 20 square matrix

Step twelve: Compute matrix **0** where matrix **0** is a 18 x 1 column vector of 0

Step thirteen: Compute **β'** where **β'** is a composite matrix (**β**, **0**, **0**).

Step fourteen: Compute **f'** using Equation (24) for each value of **C^M**

Step fifteen: Compute **C^c(t)** using Equation (6) which is solved by Simpson's numerical method of integration

Step sixteen: Calculate **r(t)** using equation $r(t) = \int f(t)dt$ using Simpson's numerical method

Steps one to sixteen is carried out by MATLAB software package by imputing different mole fractions of each of the exit streams at the respective temperatures.

Simulated results for the conversion of concentration time data to reaction rate data are presented in the following forms:

- (a) Graph of rate versus concentration at each temperature for n-hexane in the exit stream
- (b) Graph of back calculated concentration against measured concentration for each component in the exit stream at different temperatures.

6.1.1 Aromatization of n-hexane on Platinum/Alumina catalyst at temperature 440°C

Figure 1a shows a linear relationship between the reaction rate and concentration of n-hexane at temperature 440°C. The best model which fits the description of the catalytic reforming of n-Hexane over Platinum/Alumina Catalyst, after discriminating it among many other models is given as:

$$-r_5 = \frac{\frac{K_{5r}K_{1f}K_{4f}K_{10f}^2[N]}{[H_2]} - \frac{K_{5r}[H_2]^3[B]}{K_{6f}K_{7f}K_{8f}K_{9f}K_{10f}^6}}{1 + K_{1f}[N] \left(1 + \frac{K_{4f}K_{10f}^2}{[H_2]}\right) + \frac{[CP]}{K_{3f}} + \frac{[H_2]^2[B]}{K_{8f}K_{9f}K_{10f}^4} \left(\frac{[H_2]}{K_{6f}K_{7f}K_{10f}^2} + \frac{1}{K_{7f}} + 1\right) + \frac{[B]}{K_{9f}} + \frac{[H_2]^{1/2}}{K_{10f}}} \quad (25)$$

The parameters in this model are obtained by the Nelder-Mead Simplex method of multivariable optimization. The best fit Equation (25) is shown in Figure 1a as a smooth curve in which the rate of reaction increases smoothly to 3.63589ml/mg.min as the concentration of n-hexane in exit stream changes from 0.379 to 0.372gmol/m³ in a non-linear fashion. The time-concentration profile back calculated from the best-fit rate equation is shown as a continuous curve in Figure 1b. Good correlation is seen between the calculated concentration and the measured concentration of n-hexane.

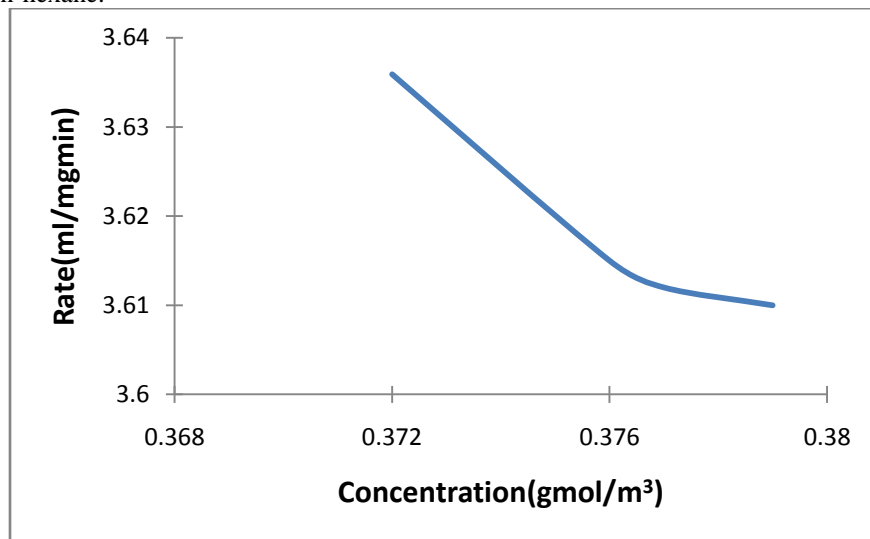


Figure 1a: Graph of measured concentration of n-Hexane in exit stream versus rate at 440°C

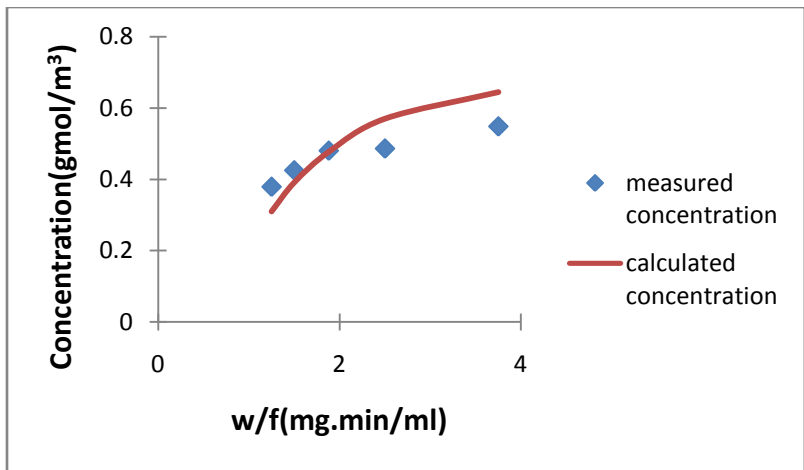


Figure 1b: Experimental concentration, calculated concentration versus time for n-hexane at 440°C

6.1.2 Aromatization of n-hexane on Platinum/Alumina catalyst at temperature 460°C

Figure 2a shows a linear relationship between the reaction rate and Concentration of n-Hexane in exit stream at temperature 460°C.

The best fit Equation (25) is shown in Figure 2a as a smooth curve in which the rate of reaction decreases smoothly to -0.62657ml/mg.min as the concentration of n-hexane in exit stream changes from 0.416 to 0.743gmol/m³ in a non-linear fashion. The time-concentration profile back calculated from the best-fit rate equation is shown as a continuous curve in Figure 2b. Good correlation is seen between the calculated concentration and the measured concentration of n-hexane.

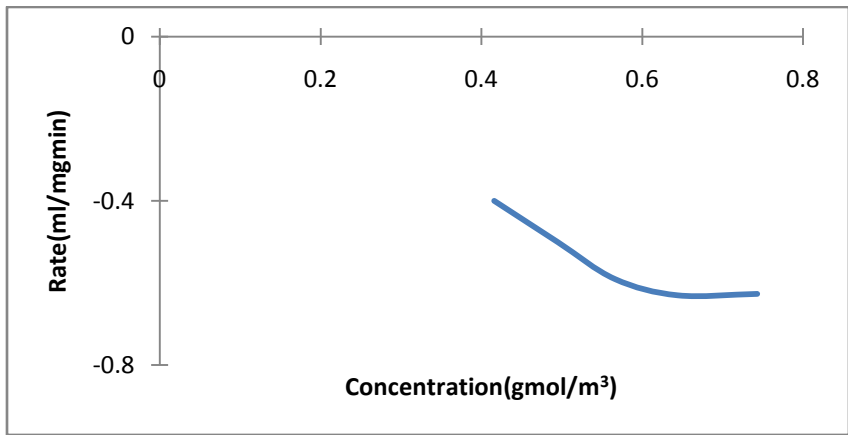


Figure 2a: Measured concentration of n-Hexane in exit stream versus rate at 460°C

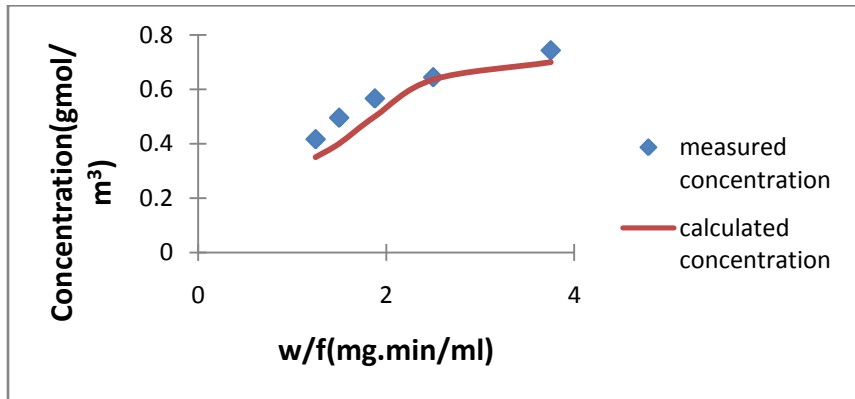


Figure 2b: Experimental concentration, calculated concentration versus time for 2-hexane at 460°C

6.1.3 Aromatization of n-hexane on Platinum/Alumina catalyst at temperature 480°C

Figure 3a shows a linear relationship between the reaction rate and concentration of n-hexane in exit stream at temperature 480°C. The best fit Equation (25) is shown in Figure 3a as a smooth line in which the rate of reaction increases smoothly to 2.91272ml/mgmin as the concentration of n-hexane in exit stream changes from 0.2610 to 0gmol/m³ in a linear fashion. The time-concentration profile back calculated from the best-fit rate equation is shown as a continuous curve in Figure 3b. Good correlation is seen between the calculated concentration and the measured concentration of n-hexane.

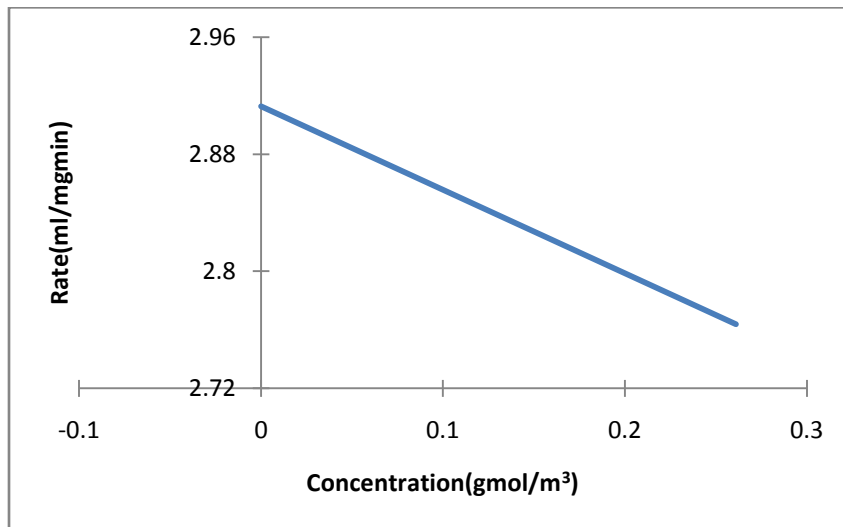


Figure 3a: Measured concentration of n-hexane in exit stream versus rate at 480°C

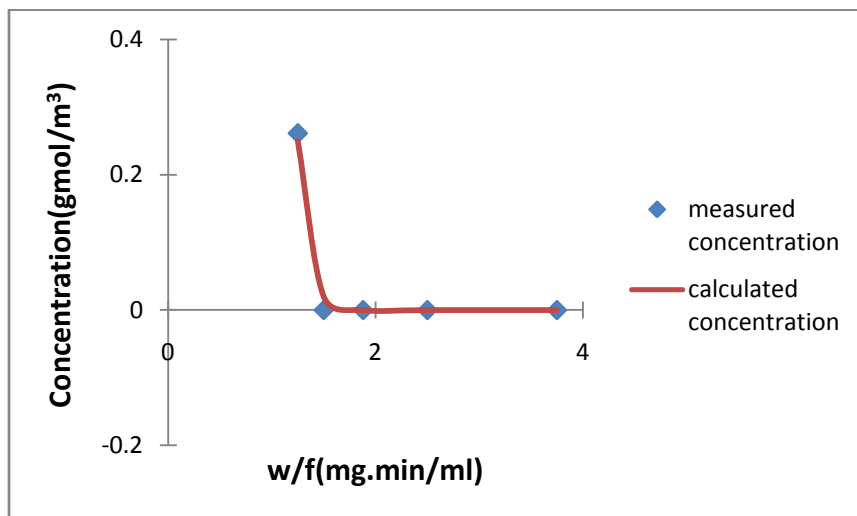


Figure 3b: Experimental concentration, calculated concentration versus time for n-hexane at 480°C

6.1.4 Aromatization of n-hexane on Platinum/Alumina catalyst at temperature 500°C

Figure 4a shows a linear relationship between the reaction rate and concentration of n-hexane in exit stream at temperature 500°C. The concentration of n-hexane in the exit stream is 0gmol/m³ which implies all the n-hexane coming into the reaction is completely converted. The best fit Equation (25) is shown in Figure 4a as a smooth line in which the rate of reaction is constantly at 0ml/mg.min. The time-concentration profile back calculated from the best-fit rate equation is shown as a continuous line in Figure 4b. Good correlation is seen between the calculated concentration and the measured concentration of n-hexane.

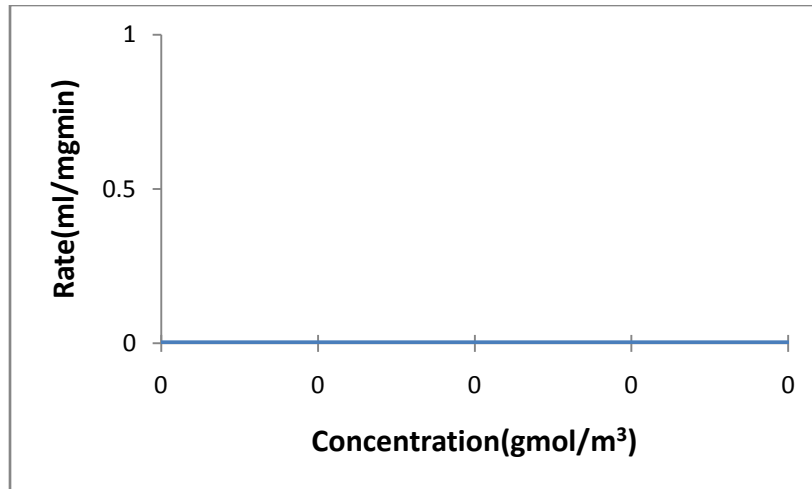


Figure 4a: Measured concentration of n-hexane in exit stream versus rate at 500°C

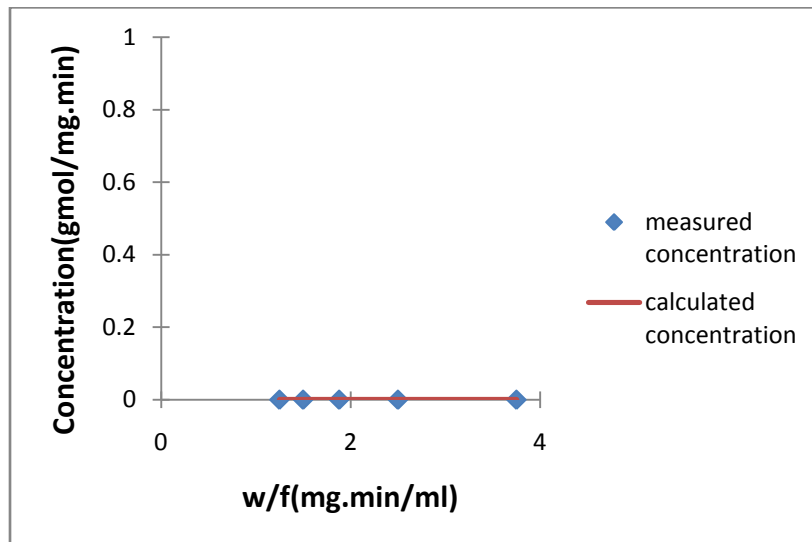


Figure 4b: Experimental concentration, calculated concentration versus time for n-hexane at 500°C

7. Kinetics of the Aromatization of n-hexane on Platinum/Alumina Catalyst

The reforming of n-Hexane on Pt/Al₂O₃ is proposed to undergo the following steps

1. $N + S \rightleftharpoons NS$ $K_1 = K_N = \frac{K_{1f}}{K_{1r}}$ (26)
2. $NS \rightleftharpoons CPS$ $k_2 = k_{Na} = \frac{k_{2f}}{K_{2r}}$ (27)
3. $CPS \rightleftharpoons CP + SK_3 = K_{CP} = K_{3f}/K_{3r}$ (28)
4. $NS + 2S \rightleftharpoons N^-S + 2HS$ $K_4 = K_N^a = K_{4f}/K_{4r}$ (29)
5. $N^-S \rightleftharpoons MSK_5 = K_{N^-} = K_{5f}/K_{5r}$ (30)
6. $MS + 2S \rightleftharpoons M^-S + 2HSK_6 = K_M = \frac{K_{6f}}{K_{6r}}$ (31)
7. $M^-S \rightleftharpoons L^-SK_7 = K_{M^-} = \frac{K_{7f}}{K_{7r}}$ (32)
8. $L^-S + 4S \rightleftharpoons BS + 4HS$ $K_8 = K_{L^-} = \frac{K_{8f}}{K_{8r}}$ (33)
9. $BS \rightleftharpoons B + S$ $K_9 = K_B = \frac{K_{9f}}{K_{9r}}$ (34)



The site balance is

$$1 = S + NS + CPS + N^-S + MS + M^-S + L^-S + BS + HS \quad (36)$$

The construction of model 1 is based on the assumption that adsorption of n-Hexane is the rate determining step while other elementary reactions are in quasi-equilibrium.

$$r_1 = K_{1f}[NS] - K_{1r}[N][S] \quad (37)$$

$$r_1 = \frac{\frac{K_{1f}[CP]}{K_2K_3} - K_{1r}[N]}{1 + \frac{[CP]}{K_2K_3} \left(\frac{1}{K_2} + 1 \right) + \frac{K_4K_{10}^2[CP]}{K_2K_3[H_2]} \left(1 + K_5 + \frac{K_5K_6K_{10}^2}{[H_2]} + \frac{K_5K_6K_7K_{10}^2}{[H_2]} \right) + \frac{[B]}{K_9} + \frac{[H_2]^{\frac{1}{2}}}{K_{10}}} \quad (38)$$

The construction of model 2 is based on the assumption that conversion of adsorbed n-Hexane to Hexene-1 is rate determining. The rate expression is:

$$r_4 = K_{4f}[N^-S][HS]^2 - K_{4r}[NS][S] \quad (39)$$

$$r_4 = \frac{\frac{K_{4f}[H_2]^4[B]}{K_5K_6K_7K_8K_9K_{10}^8} - K_{4r}K_1[N]}{\left[1 + K_1[N] + \frac{[CP]}{K_3} + \frac{[H_2]^2[B]}{K_8K_9K_{10}^4} \left(\frac{[H_2]}{K_5K_6K_7K_{10}^2} + \frac{[H_2]}{K_6K_7K_{10}^2} + \frac{1}{K_7} + 1 \right) + \frac{[B]}{K_9} + \frac{[H_2]^{\frac{1}{2}}}{K_{10}} \right]^3} \quad (40)$$

Model 3 is based on the assumption that the conversion of adsorbed hexene-1 to adsorbed Methylcyclopentane is rate determining

$$r_5 = K_{5f}[MS] - K_{5r}[N^-S] \quad (41)$$

$$r_5 = \frac{\frac{K_{5f}[B]}{K_6K_7K_8K_9K_{10}^6} - \frac{K_{5r}K_1K_4K_{10}^2[N]}{[H_2]}}{1 + K_1[N] \left(1 + \frac{K_4K_{10}^2}{[H_2]} \right) + \frac{[CP]}{K_3} + \frac{[H_2]^2[B]}{K_8K_9K_{10}^4} \left(\frac{[H_2]}{K_6K_7K_{10}^2} + \frac{1}{K_7} + 1 \right) + \frac{[B]}{K_9} + \frac{[H_2]^{\frac{1}{2}}}{K_{10}}} \quad (42)$$

Model 4 is based on the assumption that the conversion of adsorbed methylcyclopentane to adsorbed methylcyclopentene

$$r_6 = k_{6f}[M^-S][HS]^2 - K_{6r}[MS][S]^2 \quad (43)$$

$$r_6 = \frac{\frac{k_{6f}[H_2]^3[B]}{K_7K_8K_9K_{10}^6} - \frac{K_{6r}K_1K_4K_5K_{10}^2[N]}{[H_2]}}{\left[1 + K_1[N] + \frac{K_1K_4K_{10}^2[N]}{[H_2]} (1 + K_5) + \frac{[CP]}{K_3} + \frac{[H_2]^2[B]}{K_8K_9K_{10}^4} \left(\frac{[H_2]}{K_6K_7K_{10}^2} + \frac{1}{K_7} + 1 \right) + \frac{[B]}{K_9} + \frac{[H_2]^{\frac{1}{2}}}{K_{10}} \right]^3} \quad (44)$$

Model 5 is based on the assumption that the conversion of adsorbed methylcyclopentene to adsorbed cyclohexene is rate determining.

$$r_7 = k_{7f}[L^-S] - k_{7r}[M^-S] \quad (45)$$

$$r_7 = \frac{\frac{k_{7f}[H_2]^2[B]}{K_8K_9K_{10}^4} - \frac{K_{7r}K_1K_5K_6K_{10}^4[N]}{[H_2]^2}}{1 + K_1[N] + \frac{K_1K_4K_{10}^2[N]}{[H_2]} \left(1 + K_5 + \frac{K_5K_6}{[H_2]} \right) + \frac{[CP]}{K_3} + \frac{[H_2]^2[B]}{K_8K_9K_{10}^4} + \frac{[B]}{K_9} + \frac{[H_2]^{\frac{1}{2}}}{K_{10}}} \quad (46)$$

Model 6 is based on the assumption that the conversion of adsorbed cyclohexene to adsorbed benzene is rate determining.

$$r_8 = K_{8f}[BS][HS]^4 - K_{8r}[L^-S][S]^4 \quad (47)$$

$$r_8 = \frac{\frac{k_{8f}[B]}{K_9K_{10}^4} - \frac{K_{8r}K_1K_4K_5K_6K_7K_{10}^4[N]}{[H_2]^2}}{1 + K_1[N] + \frac{K_1K_4K_{10}^2[N]}{[H_2]} \left(1 + K_5 + \frac{K_5K_6K_{10}^2}{[H_2]} + \frac{K_5K_6K_7K_{10}^2}{K_7} \right) + \frac{[CP]}{K_3} + \frac{[B]}{K_9} + \frac{[H_2]^{\frac{1}{2}}}{K_{10}}}^5 \quad (48)$$

Model 7 is based on the assumption that the conversion of adsorbed benzene to benzene is rate determining.

$$r_9 = k_{9f}[B][S] - K_{9r}[BS] \quad (49)$$

$$r_9 = \frac{k_{9f}[B] - \frac{K_{9r}K_1K_4K_6K_7K_8K_{10}^8[N]}{[H_2]^4}}{1 + K_1[N] + \frac{K_1K_4K_{10}^2[N]}{[H_2]} \left(1 + K_5 + \frac{K_5K_6K_{10}^2}{[H_2]} + \frac{K_5K_6K_7K_{10}^2}{[H_2]} + \frac{K_5K_6K_7K_8K_{10}^6}{[H_2]^4} \right) + \frac{[CP]}{K_3} + \frac{[H_2]^{\frac{1}{2}}}{K_{10}}} \quad (50)$$

Model 8 is based on the assumption that the conversion of adsorbed Hydrogen to Hydrogen is rate determining.

$$r_{10} = k_{10f}[H_2]^{1/2}[S] - k_{10r}[HS] \tag{51}$$

$$r_{10} = \frac{K_{10f}[H_2]^{1/2} - \frac{K_{10r}[H_2]^{1/2}}{K_{10f}}}{1 + K_{1f}[N] + \frac{K_{1f}K_{4f}K_{10f}^2[N]}{[H_2]} \left(1 + K_{5f} + \frac{K_{5f}K_{6f}K_{10f}^2}{[H_2]} + \frac{K_{5f}K_{6f}K_{7f}K_{10f}^2}{[H_2]} + \frac{K_{5f}K_{6f}K_{7f}K_{8f}K_{10f}^6}{[H_2]^4} \right) + \frac{[CP]}{K_{3f}} + \frac{[H_2]^{1/2}}{K_{10f}}} \tag{52}$$

8. PARAMETER ESTIMATION AND OPTIMIZATION TECHNIQUE

Estimating the kinetic parameters of a rate model is a very important aspect of any kinetic investigation. This can be accomplished by least-square fitting of the rate equation into the concentration-reaction rate curve. The polyhedron method of Nelder and Mead is used to achieve this using FORTRAN software package.

The general objective in optimization is to choose a set of values of variables (or parameters) subject to the various constraints that produce the desired optimum response for the chosen objective function [5]. For the polyhedron method of Nelder and Mead used in this investigation, the objective function is the sum of squares of residuals between experimental and predicted rates of reaction.

$$S = \sum_{i=1}^n (r_i^{calc} - r_i^{obs})^2 \tag{53}$$

The smaller the value of S, the better the model and the more reliable the values of the kinetic parameters thus obtained. This method incorporates portions of the polyhedron method with the additional advantage of not restricting intermediate iteration to the feasible region. This method alters the shape of the simplex to suit local topology. The tolerance criterion is reduced within the region of an optimum till it reaches a preset small value. The results for the kinetic parameters estimated for each of the models is presented as tables 1-8

Table 1: kinetic parameters and objective functions for model I

	TEMPERATURE (°C)			
	440	460	480	500
K_{1f}	2.075E+04	3.228E+01	7.493E+00	5.000E+01
K_{1r}	1.521E+05	3.551E+00	1.443E+00	5.072E+00
$K_1(K_{1f}/ K_{1r})$	1.364E-01	9.090E+00	5.193E+00	9.858E+00
K_2	6.605E+04	2.941E+01	2.3480E+01	2.551E+01
K_3	7.151E+04	1.089E+01	7.882E+00	1.107E+01
K_4	8.380E+04	8.724E+00	9.001E+00	7.214E+00
K_5	2.239E+03	2.549E+00	2.689E+00	2.560E+00
K_6	1.493E+05	5.743E+00	4.598E+00	4.865E+00
K_7	-4.574E+05	4.313E+00	4.489E+00	5.172E+00
K_9	6.856E+04	7.321E+00	6.412E+00	3.270E+00
K_{10}	3.561E+04	1.017E+01	9.841E+00	1.021E+01
<i>Objective function</i>	-0.4574443E+06	6.945E-05	4.2782E-05	1.4039E-05

Table2: kinetic parameters and objective functions for model II

	TEMPERATURE (°C)			
	440	460	480	500
K_{4f}	2.125E+02	7.661E+00	4.374E+01	4.022E+01
K_{4r}	7.776E+01	7.607E+00	7.407E+00	7.000E+00

K_4	2.732E+00	1.007E+00	5.906E+00	5.746E+00
K_1	3.268E+01	1.350E+00	2.589E+00	1.447E+00
K_3	3.684E+01	2.325E+00	6.120E+00	5.789E+00
K_5	3.991E+01	4.632E+00	9.641E+00	7.231E+00
K_6	-9.234E-01	1.477E+01	2.198E+01	1.344E+01
K_7	3.183E+02	1.866E+01	2.476E+01	2.065E+01
K_8	5.554E+01	2.068E+01	3.391E+01	2.355E+01
K_9	1.360E+02	2.486E+01	3.778E+01	2.777E+01
K_{10}	8.508E+01	2.794E+01	4.161E+01	3.130E+01
<i>Objective Function</i>	5.554091E+01	5.670E-01	3.410E-01	8.920E-01

Table 3: Kinetic parameters and objective functions for model III

	TEMPERATURE (°C)			
	440	460	480	500
K_{5f}	6.444E+02	8.209E+02	9.508E+02	9.600E+02
K_{5r}	3.487E+03	5.305E+03	7.124E+03	9.068E+02
K_5	1.848E-01	1.515E-01	1.334E-01	1.059E+00
K_1	1.512E+03	0.005E+00	3.500E-02	3.900E+00
K_3	-7.131E+02	2.222E+02	1.721E+02	2.045E+01
K_4	1.654E+03	2.632E+02	2.537E+02	3.500E+00
K_6	1.908E+03	3.816E+02	3.774E+02	2.777E+01
K_7	4.851E+01	1.338E+02	1.089E+02	3.130E+01
K_8	3.668E+03	1.333E+02	1.127E+02	3.891E+00
K_9	-1.022E+04	2.016E-03	2.092E-03	8.890E-01
K_{10}	1.681E+03	4.199E-02	7.320E-02	3.760E-04
<i>Objective function</i>	-1.0221E+04	2.8310E-09	2.899E-09	1.447E+00

Table 4: Kinetic parameters and objective functions for model IV

	TEMPERATURE (°C)			
	440	460	480	500
K_{6f}	2.125E+02	1.440E-01	2.200E-01	2.870 E-01
K_{6r}	7.776E+02	6.170E-01	0.542 E-01	7.210E-01
K_6	2.732E+00	2.333E-01	4.059E+00	3.980E-01
K_1	3.268E+01	2.780E-01	0.169 E-01	1.610 E-01
K_3	3.684E+01	6.700E-01	0.239 E-01	6.340 E-01
K_4	3.991E+01	2.610E-01	0.106 E-01	2.180 E-01
K_5	-9.234E-01	7.300E-01	0.184 E-01	2.940 E-01
K_7	3.183E+02	1.280E-01	0.041 E-02	6.390 E-01
K_8	5.554E+01	3.920E-01	0.111 E-01	1.990 E-01
K_9	1.360E+02	8.010E-01	0.135 E-01	7.550 E-01
K_{10}	8.508E+01	2.300E-01	0.445 E-01	4.000 E-01
<i>Objective function</i>	5.554091E+01	4.921E-02	4.544 E-04	4.544 E-04

Table 5: Kinetic parameters and objective functions for model V

	TEMPERATURE (°C)			
	440	460	480	500
K_{7f}	2.075E+04	4.355 E+01	4.218 E+01	1.028E+02

K_{7r}	1.521E+05	2.521 E+00	1.041 E+00	7.092E+01
K_7	1.364E-01	1.727E+01	4.052E+01	1.449E+00
K_1	6.605E+04	7.858E+01	9.552E+01	9.997E+01
K_3	7.151E+04	4.729E+01	2.894E+01	2.088E+01
K_4	8.380E+04	4.889E+01	5.279E+01	6.017E+01
K_5	2.239E+03	2.728E+01	1.500E-02	0.089E-02
K_6	1.493E+05	4.025E+01	5.548E+01	1.097E+02
K_8	-4.574E+05	4.340E+01	6.678E+01	6.345E+01
K_9	6.856E+04	2.9167E+01	3.636E+01	1.237E+01
K_{10}	-3.561E+04	2.3435E+01	2.735E+01	2.265E+01
<i>Objective function</i>	-4.574443E+05	4.270E+02	9.23 E-05	5.410E-05

Table6: kinetic parameters and objective functions for model VI

	TEMPERATURE (°C)			
	440	460	480	500
K_1	2.080E+02	1.363 E+01	1.3740 E+01	1.3740 E+01
K_3	5.008E-01	4.755E+00	4.990 E+00	4.990 E+00
K_4	1.180E+02	2.810E+00	2.754E+00	2.754E+00
K_1	1.243E-01	1.270E+00	1.757 E+00	1.757 E+00
K_3	8.537E-01	8.584E+01	8.5700 E+01	8.5700 E+01
K_4	5.000E-03	6.760E+01	6.7480 E+01	6.7480 E+01
K_5	1.705E+00	5.6810 E+01	5.6810 E+01	5.6810 E+01
K_6	2.406E+02	5.366E+01	5.343 E+01	5.343E+01
K_7	3.000E+02	8.590 E+01	8.570 E+01	8.570E+01
K_9	1.000E+02	5.710E+01	5.681 E+01	5.681E+01
K_{10}	1.000E+02	1.584E+01	1.533 E+01	1.533E+01
<i>Objective function</i>	1.000E+01	2.600E-03	2.646 E-01	4.01E-02

Table7: kinetic parameters and objective functions for model VII

	TEMPERATURE (°C)			
	440	460	480	500
K_{9f}	2.075E+04	6.943E+00	7.611 E+01	7.290 E+01
K_{9r}	1.521E+05	3.661 E+00	3.543 E+01	3.524 E+01
K_9	1.364E-01	1.896E+00	2.150E-01	2.069E+00
K_1	6.605E+04	1.450E+00	1.580E+01	1.443 E+00
K_3	7.151E+04	1.276E+01	1.141E+01	1.149 E+01
K_4	8.380E+04	1.413E+01	1.481E+01	1.755 E+01
K_5	2.239E+03	1.977E+01	16.980E+01	2.354 E+01
K_6	1.493E+05	2.126E+01	2.176 E+01	2.865 E+01
K_7	-4.574E+05	2.860E+01	26.905 E+01	3.145 E+01
K_8	6.856E+04	3.086E+01	30.782 E+01	3.477 E+01
K_{10}	-3.561E+04	3.607 E+00	3.707 E+00	1.600 E+00
<i>Objective function</i>	-4.574443E+05	5.470 E-01	3.710 E-01	8.420 E-01

Table8: kinetic parameters and objective functions for model VIII

	TEMPERATURE (°C)			
	440	460	480	500
K_{10f}	7.375 E+00	7.691 E+00	7.543 E+01	6.624 E+01

K_{10r}	1.560 E+00	2.907 E+00	3.707 E+01	3.610 E+01
K_1	1.701E+00	1.550E+00	1.590E+00	1.493E+00
K_3	1.481E+01	1.112 E+01	1.491E+01	1.157 E+01
K_4	1.731 E+01	1.572 E+01	1.858 E+01	1.694 E+01
K_5	2.024 E+01	1.825 E+01	2.177 E+01	1.825 E+01
K_6	2.347 E+01	2.063 E+01	2.391 E+01	2.375 E+01
K_7	2.644 E+01	2.488 E+01	2.878 E+01	2.687 E+01
K_8	2.999 E+01	2.794 E+01	3.261 E+01	29.390 E+01
Objective function	3.520E-01	5.470E-01	3.710E-01	8.620E-01

9. DISCUSSION

Tikhonov regularization computation has been applied to the experimental time-conversion of n-hexane aromatization on Pt/Al₂O₃ at a temperature range of 440-500°C in hydrogen carrier. Eq. (24) was used to perform all the data conversion. The data as generated by Eq. (24)

are in the form of a discrete set of reaction rate data points at uniformly and closely spaced time intervals. These discrete data points, without assuming any rate model, were used to back calculate the time-concentration profiles. The back-calculated profiles, for all the examples considered, are in good agreement with the original experimental data. As the back calculations were performed using commercial software independent of that developed for the Tikhonov computation, they provide a quick check against possible errors introduced during the derivation and solution of Eq. (24).

The outcome of the Tikhonov regularization computation can now be put in the form of a set of closely spaced concentration versus reaction rate points. As can be seen from figures 1a, 2a, 3a&4a, the best fit Eq. (42) is shown as a smooth curve in which the rate of reaction changes as the concentration of n-hexane in exit stream changes in a non-linear fashion.

The smooth curves were used to determine the parameters in the models. Irrespective of the nature of the reaction, the key step involved is the fitting of the rate expression of the model to the well-behaved concentration-rate curve. This was accomplished by the flexible tolerance search method. Based on the behavior of these parameters, the rate models were screened in order to determine the model that fits the data best. The parameter estimates were in no means unique, but were expected to follow a general trend.

The discrimination amongst the rival models using the generated results from 8.0 is based on the following factors:

- The agreement of estimated rate constants with the expected trend of increasing rate constants as temperature increases.
- The agreement of estimated equilibrium constants with the expected trend of its decrease with temperature increase.
- The respective values of the objective function at each temperature, over the whole temperature range.
- Thermodynamic scrutiny. This involves assessing the kinetic models against the Boudart-Mears-Vannice guidelines [14,15].

This criterion is given as:

$$10 < -\Delta S_{\text{ads}} < 12.2 - 0.014\Delta H_{\text{ads}} \quad (54)$$

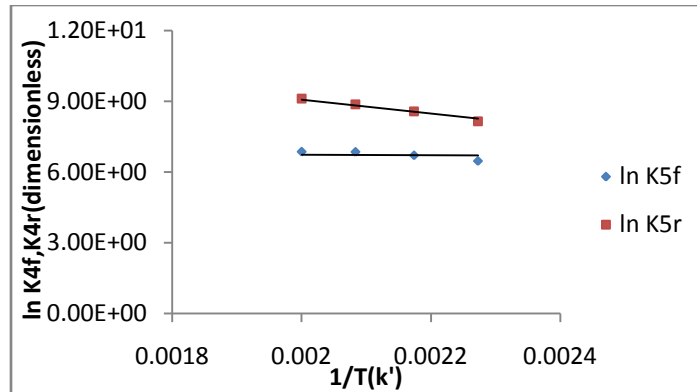
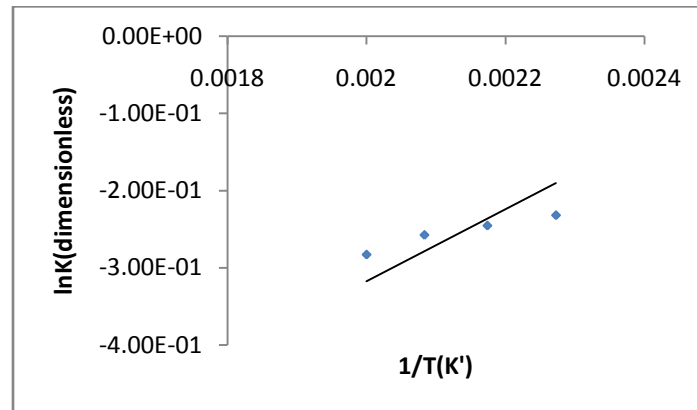
where

$$\ln K = \frac{-\Delta H}{RT} + \frac{\Delta S}{R} \quad (55)$$

The result for the estimation of the rate constants and equilibrium constants for model 3 as presented in Table 1 shows an increase in value for the rate constants of the forward and backward reaction from temperatures 440-500°C while the equilibrium constants showed a consistent decrease in value across the temperature range.

Furthermore, model 3 was tested for its thermodynamic adequacy using Eq. (54). From Figure 5 (Model 3) the plot of $\ln K$ against $1/T$ gave values for $\Delta H/R$ as the slope and $\Delta S/R$ as the intercept of the graphs respectively. The slope of the Vant Hoff plot for Model 1 is 1.6916E+08 and the intercept 5.0E+01. The slope of the Vant Hoff plot for Model 3 is 1.803357E+02 and the intercept is -1.25

Model 3 is the only model that satisfied the afore mentioned criteria. This model is the rate of conversion of adsorbed hexene-1 to adsorbed methylcyclopentane when hydrogen is adsorbed as a bi-molecular specie. From the Vant Hoff plot for this model (Fig. 5), the enthalpy of reaction, ΔH_{rxn} , for the aromatization of n-hexane was computed to be -1499.311 J/mol. The activation energy for forward and backward reaction was obtained from Figure 6 as -1.497E+03 J/mol and -3.491E+03 J/mol while the Arrhenius constants are 15s^{-1} & 7s^{-1}

Figure 6: Arrhenius plot of $\ln K_{4f}$ and $\ln K_{4r}$ against $1/T$ for Model 3Figure 5: Vant Hoff plot of $\ln K_4$ against $1/T$ for Model 3

10. CONCLUSION

In the analyses carried out on n-hexane aromatization, the similarity between the experimental data and the concentration vs. W/F data reproduced by Tikhonov regularization (Figures 1b-4b) can be considered as satisfactory, in view of the entirely different approach by which they were obtained. Therefore, Tikhonov regularization technique is a reliable procedure for converting experimental time-concentration data into concentration-reaction rate data. It does not require the assumption of a rate model to describe the experimental data and it also manages to keep noise amplification under control. Thus, it leads to a more reliable concentration-reaction rate profile and allows the kinetic parameters in the rate models to be determined with greater ease and also with a higher degree of certainty. Based on the fact that the rate constants of Model 3 increased consistently with temperature and satisfaction of the thermodynamic criterion, the assumption that the rate of conversion of adsorbed hexene-1 to adsorbed methylcyclopentane when hydrogen is adsorbed as a bi-molecular specie is the rate determining step while other reactions are in quasi equilibrium best describes the process of n-hexane aromatization.

11. NOMENCLATURE

- A** ND x N_k matrix of coefficient of unknown column vector f
- α_{ij}** A coefficient arising from the numerical integration of equation (2)
- β** A tri-diagonal matrix of coefficients arising from the finite difference approximation of d^2f/dt^2
- C_i, B_i** The coefficients of C_0 and r_0 representing the column matrices C and B respectively
- C^c** Computed Concentration
- C^M** Experimentally measured concentration
- $C(t)$** Concentration at specific time t
- C_0** Initial concentration
- δ_i** The deviation of C^c from C^M
- N_D** Number of data points
- N_k** Number of Uniformly-spaced discretization points
- $r(t)$** Rate of reaction

r_0	Initial rate of reaction
S	The objective function
t	Time
t_i	The times at which the concentration is measured
λ	The regularization parameter
x	Conversion
N	N-Hexane
Σ	Summation
N	2-hexane
CP	Cracked products
B	Benzene
M	Methylcyclopentane
T	Toluene
N'	N-Hexene
M'	Methylcyclopentene
L'	Cyclohexene
S	Vacant site on catalyst surface
s	subscript denoting adsorbed specie on the catalyst
K_f	Rate constant of forward reaction
K_r	Rate constant of reverse reaction
K	Equilibrium constant
$^{\circ}C$	Unit of Temperature in Celsius
ΔH	Enthalpy of reaction
ΔS	Entropy change for the reaction

12. REFERENCES

- [1]. K.A. Connors. Chemical Kinetics: The Study of Reaction Rates in Solution, New York: VCH, 1990.
- [2]. H.W. Engl, M. Hanke and A. Neubauer. Regularization of Inverse Problems, Dordrecht: Kluwer Academic Publishers, 2000.
- [3]. Y. L. Yeow, S. R. Wickramasinghe, B. Han, Y. Leong. A new method of processing the time-concentration data of reaction kinetics, Chemical Engineering Science 58 (2003) 3601 – 3610.
- [4]. Y.L. Yeow and J.W. Taylor. Obtaining the Shear Rate Profile of Steady Laminar tube flow of Newtonian and non-Newtonian Fluids from Nuclear Magnetic Resonance Imaging and Laser Doppler Velocimetry Data. J. Rheology, 2002, 46(2): 351–365.
- [5]. S.C. Omowunmi, A.A. Susu. Application of Tikhonov Regularization Technique to the Kinetic Data of an Autocatalytic Reaction: Pyrolysis of N-Eicosane. Engineering, 2011, 3: 1161-1179.
- [6]. A.A. Susu and T. Kunugi. Novel Pyrolysis Decomposition of n-Eicosane with Synthesis Gas and K_2CO_3 -Catalyzed Shift Reaction. I & EC Process Design & Development, 1980, 19: 693-699.
- [7]. S.C. Omowunmi and A.A. Susu. Application of Tikhonov Regularization Technique to the Kinetic Analysis of N-Heptane, 2-Heptene and 3-Methylhexane Reforming on Pt/Al_2O_3 Catalysts. J. Engineering Technology Research, 2012, 1 (1): 1-18.
- [8]. D.O. Agbajelola and F. Aberuagba. Kinetic Analysis of N-Hexane Aromatization on Pt/Alumina Catalyst in Hydrogen.. International Journal of Engineering Science, 2009, 1(2), 51-58.
- [9]. J. Hadamard. Sur les problèmes aux dérivées partielles et leur signification physique. Princeton University Bulletin, 1902, 13: 49-52
- [10]. W.T. Shaw and J. Tigg. Applied Mathematica. Reading, MA, Addison-Wesley: Toledo, 1994.
- [11]. P.C. Hansen. Analysis of Discrete Ill-posed Problems by means of the L-curve'', SIAM Reviews, 1992, 34: 561–580.
- [12]. P.C. Hansen and D.P. O'Leary. The Use of the L-curve in the Regularization of Discrete Ill- Posed Problems, SIAM J. Sci. Comput., 1993, 14(6): 487–1503.
- [13]. C.L. Lawson and R.J. Hanson. Solving Least Squares Problems, Englewood Cliffs, NJ: Prentice-Hall, 1974.
- [14]. M. Boudart, D.E. Mears and M. A. Vannice. Kinetics of Heterogeneous Catalytic Reactions, IndustrieChimiqueBelge, 1967, 32(I): 281.
- [15]. M.A. Vannice, S. H. Hyun, B. Kalpakci and W.C. Liauh. Entropies of Adsorption in Heterogeneous Catalytic Reactions, 1979, Journal of Catalysis 56: 358.
- [16]. N.Groetsch. The Theory of Tikhonov Regularization for Fredholm Integral Equations of the First Kind, London: Pitman, 1984.